# Excitation energy dependence of the level density parameter close to the doubly magic $^{208}$Pb

Pratap Roy,[1,2,*] K. Banerjee,[1,2] C. Bhattacharya,[1,2] R. Pandey,[1] A. Sen,[1] S. Manna,[1,2] S. Kundu,[1,2] T. K. Rana,[1] T. K. Ghosh,[1,2] G. Mukherjee,[1,2] T. Roy,[1,2] A. Dhal,[1] A. Dey,[1] J. K. Meena,[1] A. K. Saha,[1] Deepak Pandit,[1] S. Mukhopadhyay,[1,2] and S. Bhattacharya[1]

[1]*Variable Energy Cyclotron Centre, HBNI, 1/AF, Bidhan Nagar, Kolkata - 700064, India*

[2]*Homi Bhabha National Institute, Training School Complex, Anushaktinagar, Mumbai - 400094, India*

(Received 21 October 2016; published 12 December 2016)

Neutron evaporation spectra have been measured from $^{4}$He + $^{208}$Pb and $^{4}$He + $^{209}$Bi reactions by using $^{4}$He-ion beams of several bombarding energies. Excitation-energy dependence of the level density parameter has been studied for the two systems in the excitation energy range of ~18–50 MeV. For both the reactions an overall reduction of the asymptotic level density parameter with increasing excitation energy (temperature) is observed. The trend of the data was compared with the Thomas–Fermi model predictions and found to be in reasonable agreement. The value of the shell damping parameter has been extracted from the lowest-energy data in the case of $^{210,211}$Po and $^{211,212}$At nuclei close to the $Z = 82$ and $N = 126$ shell closure, and it was found to be consistent with the recent measurement in the vicinity of doubly magic $^{208}$Pb nucleus.

DOI: 10.1103/PhysRevC.94.064607

## I. INTRODUCTION

Nuclear level density (NLD), which is the most important input to the statistical model description of various nuclear reactions, has been a matter of investigation over a long time. Understanding the nature of variation of NLD on various factors such as excitation energy, angular momentum, pairing, shell corrections, deformation, isospin, parity, etc. is crucial from both fundamental and application points of view. In some of our recent studies important information on the dependence of NLD on angular momentum [1–3] and ground-state deformation [4] were reported. Another important factor, by which NLD is strongly influenced, is the shell structure of the atomic nuclei. Strong departure of the level density parameter (LDP) from its standard low-energy value of $\sim A/8$ is very well known for nuclei in the vicinity of closed shells. The shell structure in atomic nuclei is a manifestation of the nuclear mean field which assumes that nucleons move quasi-independently from one another inside a nucleus because of Pauli's principle. So the shell effects are strongly excitation-energy dependent, expected to be damped and finally washed out at higher excitation energies due to gradual weakening of the nuclear mean field itself. Realistic shell effects can be incorporated in an exact manner in the microscopic level density calculations either by a combinatorial or by a statistical approach. However, such rigorous microscopic calculations are extremely involved, requiring large computation time, which severely limits their applications to the analysis of experimental data. Therefore in most of the statistical model codes the level density is approximated by a simple Fermi-gas-type (FG-type) analytic expression [5] and important factors such as shell effects, pairing, collectivity, etc. are incorporated in a completely phenomenological manner through a number of adjustable parameters. The most widely used excitation-energy-dependent parametrization of the shell effect in NLD is given by [6]

$$a = \tilde{a}\left[1 - \frac{\Delta S}{U}\{1 - \exp(-\gamma U)\}\right], \tag{1}$$

where $a$ is the level density parameter and $\tilde{a}$ is its asymptotic value at the excitation energy where shell effects are depleted, leaving a smooth dependence on the mass number $A$. Here $U$ is the thermal excitation energy which contributes to the temperature, $\Delta S$ is the ground-state shell correction, and $\gamma$ is the shell damping parameter. An exact determination of $\gamma$ is important because it determines the rate at which the shell effects are depleted with increasing excitation energy. Theoretically, the procedure described by Eq. (1) is quite useful because it is easy to handle (compared with the direct enumeration of NLD using shell-model single-particle level schemes) and almost applicable for all nuclei in the nuclear chart.

Experimentally, the information on the variation of the shell effect in NLD over a wide excitation range can be obtained by measuring particle evaporation spectra from an excited compound nucleus at sufficiently low energies where the shell effect has significant contribution. However, populating nuclei at such low excitation energies through the fusion reactions is difficult due to the entrance channel Coulomb barrier. This difficulty has been overcome to an extent in a recent study by Rout *et al.,* where the authors have measured neutron evaporation spectra followed by transfer-induced fusion of $^{7}$Li on $^{205}$Tl populating particle unbound states in $^{208}$Pb [7]. Another possible solution to the problem of producing low excitation energy can be through the use of light-ion beams such as protons or $\alpha$ particles for which the Coulomb barriers are relatively small. The latter method is cleaner than the earlier method in which there may be uncertainty due to the contributions coming from different direct processes. Additionally, in the second case (complete fusion) there is no uncertainty in determining the excitation energy of the compound nucleus as compared with the case of the transfer induced fusion, where the excitation energy is determined by

*pratap_presi@yahoo.co.in

 

putting an energy gate (of width ~1–2 MeV) in the measured outgoing-particle energy spectrum. In the work of Rout *et al.* [7], the shell damping parameter has been determined in the vicinity of the doubly magic $^{208}$Pb nucleus. However, the extracted $\gamma$ value ($0.060^{+0.01}_{-0.02}$ MeV$^{-1}$) differs somewhat from the value ($0.079 \pm 0.007$ MeV$^{-1}$) extracted earlier from the neutron resonance data [8].

At this point it may be pointed out that, apart from the discussed variation of the level density parameter with excitation energy due to the shell effects (important for $T \lesssim 1$ MeV); the smooth value of the LDP also shows interesting variation with excitation energy (temperature). A reduction in the value of the smooth level density parameter with increasing temperature, from $\sim A/8$ at zero temperature to $\sim A/13$ at $T \sim 5$ MeV was reported in several experimental studies, particularly in the $A \approx 160$ mass region [9–13]. It has been recognized that the observed temperature dependence of the level density parameter can be accounted for to a good extent by taking into account the effects of the temperature dependence of the effective nucleon mass [14–18]. In a simplified calculation under the Thomas–Fermi approach (TFA) including the finite-size effects (effects due to surface and curvature), the momentum and frequency dependence of the effective mass, the effects of continuum and the shell effects, the temperature variation of the level density parameter was reported for several nuclei by Shlomo and Natowitz [17]. In a study, Fineman *et al.* [19] showed that the spectral shape of light particles emitted from $^{193}$Tl and $^{213}$Fr compound systems could be explained very well by using a modest excitation-energy-dependent parametrization of smooth LDP, based on the work of Shlomo and Natowitz [17]. However, in the same work a stronger dependence of $\tilde{a}$ was required to explain the data in case of the $^{224}$Th nucleus. A very strong energy dependence of $\tilde{a}$ (from $A/8$ at low temperature to $A/12$ at $T \sim 2.5$ MeV) has been reported by Fabris *et al.* from the measurement of $\alpha$-particle emission in $^{19}\mathrm{F}+^{181}\mathrm{Ta}$ fusion-evaporation reactions [20]. However, such a strong dependence was not supported by later measurements for the same $^{19}\mathrm{F}+^{181}\mathrm{Ta}$ system by Caraley *et al.* [21]. In the case of lighter systems [22–24], a constant nature or rather weak dependence of LDP on $T$ compared with the observations in the $A \sim 160$ region or with the predictions of Shlomo and Natowitz [17] was reported in many cases.

It is therefore evident from the above discussion that several interesting studies have been carried out in recent years to investigate the temperature dependence of the level density parameter as well as the role of shell effects and its damping on NLD. For the latter, measurements are very few and new measurements will be useful to substantiate the earlier results. On the other hand, results of different measurements on the temperature dependence of the level density parameter are so diverse that it is difficult to arrive at a definite conclusion. Therefore, we studied the energy dependence of the level density parameter and the damping of shell effects with excitation energy in the $A \sim 210$ region by using light-ion-induced reactions, which has several advantages. First, because the angular momenta populated are much less compared with heavy-ion-induced (HI-induced) reactions, the thermal excitation energy can be determined with much less uncertainty. Moreover, any significant modification in the LDP due to angular-momentum effects is less likely to occur in this case. Second, the numbers of effective decay channels are also less compared with the HI reactions; therefore, the extracted level density parameters correspond more closely to those of the nuclei of interest and are not averaged over a large number of nuclei. Thus the present study is likely to extend (and improve) the available information on the shell damping and temperature dependence of the level density parameter for systems close to the doubly magic $^{208}$Pb nucleus. With this aim we carried out the present measurement, in which neutron evaporation spectra have been measured from the two different compound nuclei $^{212}$Po and $^{213}$At populated through the reactions

$$^{4}\mathrm{He}+^{208}\mathrm{Pb} \longrightarrow {}^{212}\mathrm{Po}^{*}\ (Q = -8.95\ \mathrm{MeV}),$$
$$^{4}\mathrm{He}+^{209}\mathrm{Bi} \longrightarrow {}^{213}\mathrm{At}^{*}\ (Q = -9.25\ \mathrm{MeV})$$

in an excitation range $E^{*} \sim 18$–50 MeV. The choice of the current reactions was particularly useful to produce low excitations as both the reactions have large negative $Q$ values (~9 MeV).

## II. EXPERIMENTAL DETAILS

The experiment was carried out by using the $^{4}$He-ion beams of incident energies 28, 31, 35, 40, and 60 MeV from the K130 cyclotron at the Variable Energy Cyclotron Centre (VECC). In the experiment, two self-supporting foils of $^{208}$Pb (enriched to >99%, thickness ~4 mg/cm$^2$) and $^{209}$Bi (100% natural abundance, thickness ~1.5 mg/cm$^2$) were used as targets. The emitted neutrons were detected by using four liquid scintillator detectors placed at the laboratory angles of 90°, 105°, 120°, and 150°, at a distance of 1.5 m from the target. Energies of the emitted neutrons were measured by the time-of-flight (TOF) technique, where the starts of the TOF were taken from a 50-element $\mathrm{BaF_2}$ $\gamma$-ray detector array placed very close to the target. In converting the neutron TOF to neutron energy, the prompt $\gamma$ peak in the TOF spectrum was used as the time reference. The neutron and $\gamma$ separation were achieved by both the TOF and pulse shape measurements. The beam dump has been kept at a distance of ~3 m from the target position and shielded on all sides with layers of lead and paraffin to minimize the contribution of background neutrons coming from the beam dump. The scattered-neutron contribution was estimated by blocking the neutrons from the target reaching the detectors with the help of 30-cm-thick high-density plastic (HDP) blocks placed in between the target and the detectors. The excitation-energy-dependent efficiency, which is a very crucial parameter, was measured in the in-beam condition by using a standard $^{252}$Cf neutron source. The measured efficiencies were also compared with a Monte Carlo-based simulation [25] and found to be in good agreement. The data were collected in event-by-event mode by using a VME-based data-acquisition system.

## III. RESULTS AND DISCUSSIONS

The extracted neutron kinetic-energy spectra at different angles were converted to the center-of-mass frame; the spectral

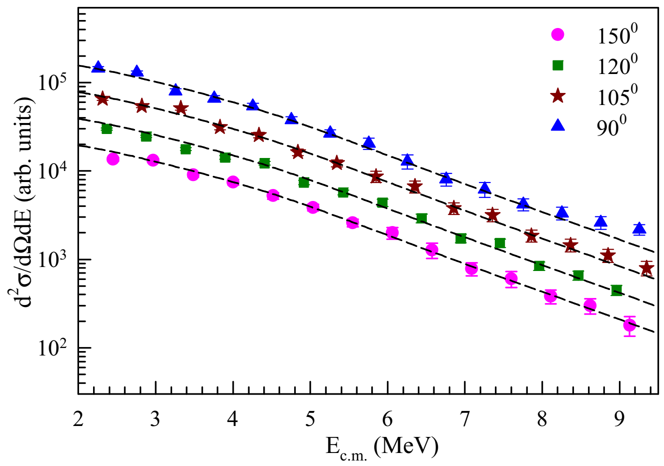


FIG. 1. The experimental neutron energy spectra (symbols) at different angles in the center-mass-frame for the $^{4}$He + $^{208}$Pb system at 60 MeV incident energy. The corresponding SM predictions are shown by dashed lines. The individual spectra have been scaled for better visualization.

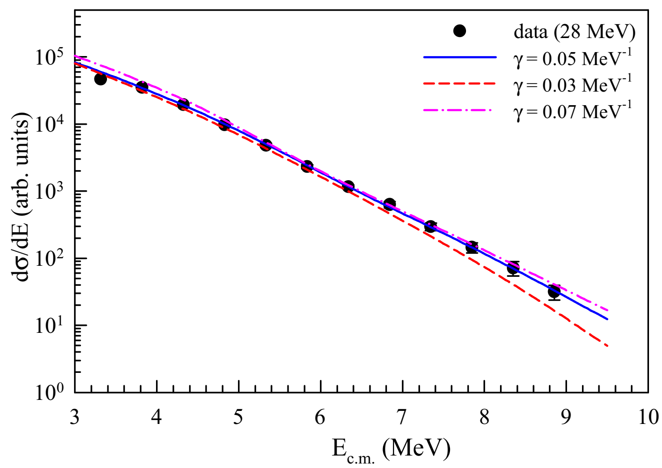


FIG. 2. The experimental neutron spectrum (symbols) along with the SM calculations (lines) using three $\gamma$ values (see text) for the $^{4}$He + $^{208}$Pb system at 28 MeV incident energy.

shapes were found to be almost overlapping (Fig. 1), indicating that they have originated from an equilibrated compound nucleus. The neutron data at the most-backward angle (150°) were used for further analysis. The experimental neutron energy spectra were compared with the theoretical calculations performed with the statistical model (SM) code CASCADE [26]. In the CASCADE calculation, the phenomenological level density formula predicted by the back-shifted Fermi gas model [5] given by

$$\rho_{\rm int}(E^*,J) = \frac{(2J+1)}{12}\left(\frac{\hbar^2}{2I_{\rm eff}}\right)^{3/2}\sqrt{a}\frac{\exp(2\sqrt{aU})}{U^2} \qquad (2)$$

was used. Here $a$ is the level density parameter and $E^*$ is the excitation energy. The thermal excitation energy $U$ is defined as

$$U = E^* - E_{\rm rot} - \Delta P, \qquad (3)$$

with the rotational energy $E_{\rm rot}$ and the pairing energy ($\Delta$P) given by

$$E_{\rm rot} = \frac{\hbar^2}{2I_{\rm eff}}J(J+1) \qquad (4)$$

and

$$\Delta P = \frac{12}{\sqrt{A}}. \qquad (5)$$

Here $I_{\rm eff} = I_0(1+\delta_1 J^2 + \delta_2 J^4)$ is the effective moment of inertia; $I_0$, $\delta_1$, and $\delta_2$ are the rigid body moment of inertia and deformability coefficients, respectively [27]. The shell correction in $a$ was incorporated through the expression given in Eq. (1). The transmission coefficients were calculated by using the optical model, where the optical model (OM) parameters were taken from Ref. [28]. It was observed that the variation in the transmission coefficients or in the angular-momentum-dependent effective moment of inertia had no significant effect on the shape of the calculated neutron evaporation spectra. The shape of the spectra was mostly determined by the value of the level density parameter $a$.

### A. Determination of the shell damping parameter

The value of shell damping parameter was extracted from the lowest-energy data ($U \sim 17$ MeV), which has the highest sensitivity (as compared with higher-energy data) for this parameter. At the lowest excitation energy both the compound nuclei $^{212}$Po and $^{213}$At decay predominately through $1n$ and $2n$ channels populating $^{211,210}$Po and $^{212,211}$At as evaporation residues (ERs), respectively, in an energy range $E^*_{\rm ER} \sim 2$–12. Over this $E^*_{\rm ER}$ range, the level density parameter is expected to show significant variation due to the damping of the shell effect. The ground-state shell corrections ($\Delta$S), which are determined from the difference between the experimental and liquid drop masses, have the values $\sim -11$ MeV for the present isotopes [29]. Figure 2 shows the measured neutron energy spectrum along with the SM predictions for the $^{4}$He on $^{208}$Pb reaction at the 28 MeV incident energy. The calculated spectra are shown for the three $\gamma$ values 0.03, 0.05, and 0.07 MeV$^{-1}$. The value of $\tilde{a}$ was taken as $A/8$ while extracting the value of $\gamma$. It can be clearly seen from Fig. 2 that $\gamma = 0.05$ describes the shape of the spectra reasonably well compared with the other two $\gamma$ values. The optimum $\gamma$ values were extracted for the two reactions by $\chi^2$ minimization and found to be $0.052 \pm 0.018$ MeV$^{-1}$(for $^{4}$He + $^{208}$Pb) and $0.054 \pm 0.020$ MeV$^{-1}$(for $^{4}$He + $^{209}$Bi). The measured values are consistent with the theoretical estimates of Refs. [6,30] and also matches with the measured value of Ref. [7]. Measurements at further lower excitation energies will be useful to constrain the value of the shell damping parameter to a narrower range. The spectral shapes at higher energies (for $E_{\rm lab} \geqslant 31$ MeV) for the current study are observed to have very little sensitivity on the variation of $\gamma$, indicating the weakening of the influence of shell effects at these energies.

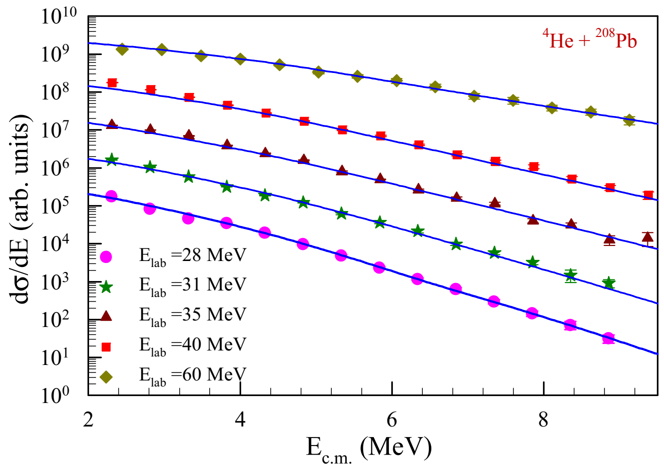


FIG. 3. Experimental neutron energy spectra (symbols) at different excitation energies along with the statistical model fits (continuous lines) for the $^4$He +$^{208}$Pb system. The individual spectra have been scaled for better visualization.

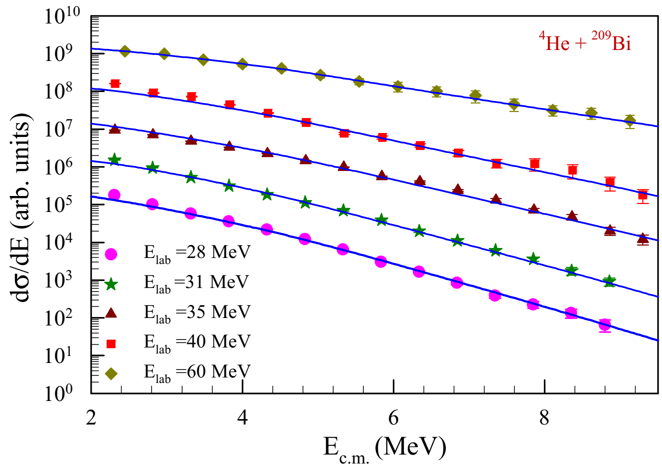


FIG. 4. Same as Fig. 3 but for the $^4$He +$^{209}$Bi system.

### B. Temperature dependence of LDP

The excitation energy (temperature) dependence of the level density parameter was studied by fitting the experimental spectra at different incident energies (shown in Figs. 3 and 4) by varying the inverse level density parameter $k$ ($k = A/\tilde{a}$). The temperature $T$ can be obtained from the relation

$$T = \sqrt{\frac{U}{a}}. \quad (6)$$

However, in the measured neutron spectra there may be contributions coming from neutrons emitted from different stages of the decay. So, the measured spectra are fitted with the Maxwellian function $\sqrt{E}e^{-\frac{E}{T}}$ to estimate the average temperatures. The extracted $k$ values along with the corresponding thermal excitation energies and temperatures are given in Table I. It can be seen from the table that the extracted temperatures from Eq. (6) and those from the Maxwell fitting are close to each other. An overall increase of the inverse level density parameter (or decrease of $\tilde{a}$) with increasing temperature is observed for both reactions. The temperature dependence of $k$ is plotted in Fig. 5 along with the theoretical prediction of Shlomo and Natowitz [17] performed under the Thomas–Fermi approach for a nucleus with $A = 210$ (continuous line in Fig. 5). It can be seen from Fig. 5 that the average trend of the data is similar to that of the TFA prediction. However, the experimental $k$ values increases at a slightly faster rate than the theoretical prediction. The experimental trend can be very well represented by an empirical relation (shown by the dashed line in Fig. 5),

$$k(U) = k_0 + \kappa \frac{U}{A}, \quad (7)$$

as used in the past by several authors to reproduce the spectral shapes of light charged particles emitted in different heavy-ion reactions in a wide-excitation-energy range [19,21,31]. The average variation of $k$ with $T$, in the current study can be explained by Eq. (7), with $k_0 = 7.8$ and $\kappa = 7.4$. The value of $\kappa$, which basically decides the rate of increase of $k$ with $U$ or $T$, agrees with the mass-number-dependent parametrization of Charity [31],

$$\kappa(A) = 0.00517e^{(0.0345A)},$$

but rather large compared with that of Ref. [17] (≈4.3 for $A = 210$). Although the current experiment could not go up to very high excitation energies as compared to the earlier

TABLE I. Extracted inverse level density parameters and temperatures.

| System | $E_{lab}$ (MeV) | $E^*$ (MeV) | $U$ (MeV) from Eq. (3) | $k$ (MeV) from the SM fit | $T$ (MeV) from Eq. (6) | $T$ (MeV) from Maxwell fitting |
|---|---|---|---|---|---|---|
| $^4$He +$^{208}$Pb | 28 | 18.5 | 16.6 | $7.8 \pm 0.4$ | 0.78 | $0.70 \pm 0.03$ |
| $^4$He +$^{208}$Pb | 31 | 21.5 | 18.8 | $8.0 \pm 0.5$ | 0.84 | $0.77 \pm 0.05$ |
| $^4$He +$^{208}$Pb | 35 | 25.4 | 21.9 | $8.5 \pm 0.3$ | 0.94 | $0.84 \pm 0.04$ |
| $^4$He +$^{208}$Pb | 40 | 30.3 | 25.8 | $8.5 \pm 0.4$ | 1.02 | $0.92 \pm 0.03$ |
| $^4$He +$^{208}$Pb | 60 | 49.9 | 44.0 | $9.5 \pm 0.4$ | 1.41 | $1.25 \pm 0.04$ |
| $^4$He +$^{209}$Bi | 28 | 18.2 | 16.3 | $8.3 \pm 0.3$ | 0.81 | $0.72 \pm 0.04$ |
| $^4$He +$^{209}$Bi | 31 | 21.2 | 18.6 | $9.0 \pm 0.4$ | 0.89 | $0.80 \pm 0.05$ |
| $^4$He +$^{209}$Bi | 35 | 25.0 | 21.5 | $9.4 \pm 0.6$ | 0.97 | $0.92 \pm 0.03$ |
| $^4$He +$^{209}$Bi | 40 | 30.0 | 25.5 | $9.5 \pm 0.4$ | 1.04 | $0.99 \pm 0.04$ |
| $^4$He +$^{209}$Bi | 60 | 49.6 | 43.7 | $10.0 \pm 0.4$ | 1.43 | $1.28 \pm 0.04$ |

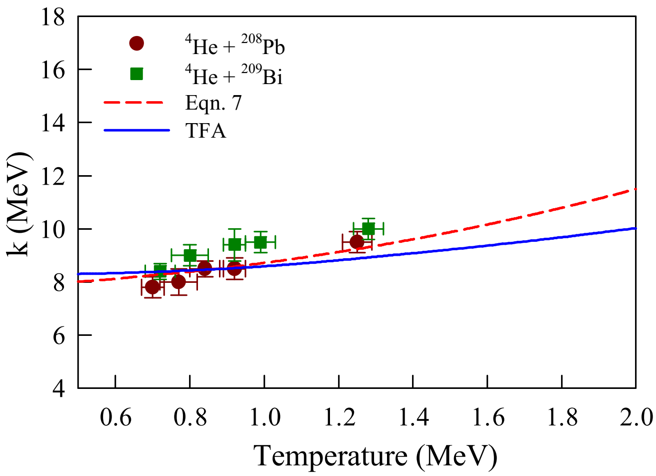


FIG. 5. Excitation-energy (temperature) dependence of the inverse level density parameter. The experimental data (symbols) are compared with the prediction of Eq. (7) (dashed line) and the TFA calculations (continuous line) of Ref. [17] (see text).

results, a clear trend could be established from the experimental data because of the precise determination of the LDP. However, more data points at higher excitation energies will always be useful to make further comments on the rate of increase of $k$ with $T$. It may be mentioned here that the reduction in the value of the asymptotic level density parameter with excitation energy can mainly be accounted for by the temperature dependence of the frequency- and momentum-dependent effective mass [17]. The frequency dependence of the effective mass, which reflects the effects of correlations, considerably enhances the surface contribution to $\tilde{a}$ at low energies, bringing it close to the observed value ($\sim A/8$) compared with the Fermi-gas prediction ($\sim A/15$) [14]. However, the effect of correlation dies out with the increase in excitation energy and the value of $\tilde{a}$ approaches its Fermi-gas limit [32]. The effect of correlation has another significant effect in NLD. Apart from increasing the value of the LDP at lower energies, the long-range correlations can also cause an enhancement of the FG level density which is known as the collective enhancement:

$$\rho_{\text{tot}}(E^*) = K_{\text{coll}}(E^*)\rho_{\text{FG}}(E^*). \quad (8)$$

Here, $K_{\text{coll}}$ is the collective enhancement factor which is a product of rotational ($K_{\text{rot}}$) and vibrational ($K_{\text{vib}}$) enhancement factors. Normally in the statistical model calculations the collective enhancement factor is not incorporated implicitly; rather an effective level density parameter is used; that is,

$$\rho_{\text{tot}}(E^*) = \rho_{\text{FG}}(E^*,\tilde{a}_{\text{eff}}) = K_{\text{coll}}(E^*)\rho_{\text{FG}}(E^*,\tilde{a}). \quad (9)$$

An increment in the value of the LDP at low energy can also be observed as a manifestation of the excitation-energy dependence of the collective enhancement factor, as recently seen in the case of nuclei having large ground-state deformations [4]. A somewhat similar observation has also been reported in the case of a relatively less deformed system in Ref. [33]. However, in the current study, all the nuclei being close to the $Z = 82$ and $N = 126$ shell closure are spherical in their ground state. Thus, the rotational enhancement factor $K_{\text{rot}} \approx 1$ [34]. Besides, the estimated vibrational enhancement factors are also quite small (1–10) for the current nuclei of interest [35]. Therefore, the contribution of the collective enhancement in the present study can safely be neglected.

## IV. SUMMARY AND CONCLUSION

The energy spectra of the neutrons emitted in the decay of $^{212}$Po* and $^{213}$At* have been measured at backward angles at $E_{\text{lab}} = 28$, 31, 35, 40, and 60 MeV and compared with the statistical model calculations. The value of the shell damping factor has been extracted from the lowest-energy data for systems close to the doubly magic $^{208}$Pb. The shell effect and its damping with increasing excitation energy was found to be well represented by the relation given in Eq. (1) with a damping parameter $\gamma = 0.052 \pm 0.018$ MeV$^{-1}$(in the case of the $^4$He $+^{208}$Pb reaction). The temperature dependence of the asymptotic level density parameter has been studied and compared with the Thomas–Fermi model calculations. An overall decrease of the LDP with increasing temperature is observed, consistent with the TFA prediction. The experimental results can also be very well explained by an linear increase of the inverse level density parameter with excitation energy, with the empirical relation, $k(U) = 7.8 + 7.4(U/A)$.

## ACKNOWLEDGMENTS

The authors are thankful to the VECC Cyclotron operators for smooth running of the accelerator during the experiment. One of the authors (S.B.) acknowledges with thanks the financial support received from the Raja Ramanna fellowship program of the Department of Atomic Energy, Government of India. One of the authors (A.D.) acknowledges with thanks the financial support provided by the Science and Engineering Research Board, Department of Science and Technology, Government of India via Project No. SR/FTP/PS067/2012.

[1] M. Gohil, Pratap Roy, K. Banerjee, C. Bhattacharya, S. Kundu, T. K. Rana, T. K. Ghosh, G. Mukherjee, R. Pandey, H. Pai, V. Srivastava, J. K. Meena, S. R. Banerjee, S. Mukhopadhyay, D. Pandit, S. Pal, and S. Bhattacharya, Phys. Rev. C **91**, 014609 (2015).

[2] K. Banerjee, S. Bhattacharya, C. Bhattacharya, M. Gohil, S. Kundu, T. K. Rana, G. Mukherjee, R. Pandey, P. Roy, H. Pai, A. Dey, T. K. Ghosh, J. K. Meena, S. Mukhopadhyay, D. Pandit, S. Pal, and S. R. Banerjee, Phys. Rev. C **85**, 064310 (2012).

[3] Pratap Roy, K. Banerjee, S. Bhattacharya, C. Bhattacharya, S. Kundu, T. K. Rana, T. K. Ghosh, G. Mukherjee, R. Pandey, J. K. Meena, M. Gohil, H. Pai, V. Srivastava, A. Dey, Deepak Pandit, S. Mukhopadhyay, S. Pal, and S. R. Banerjee, Phys. Rev. C **86**, 044622 (2012).

[4] Pratap Roy, K. Banerjee, M. Gohil, C. Bhattacharya, S. Kundu, T. K. Rana, T. K. Ghosh, G. Mukherjee, R. Pandey, H. Pai, V. Srivastava, J. K. Meena, S. R. Banerjee, S. Mukhopadhyay, D. Pandit, S. Pal, and S. Bhattacharya, Phys. Rev. C **88**, 031601(R) (2013).

[5] H. A. Bethe, Phys. Rev. **50**, 332 (1936); Rev. Mod. Phys. **9**, 69 (1937).

[6] A. V. Ignatyuk, G. N. Smirenkin, and A. S. Tishin, Sov. J. Nucl. Phys. **21**, 255 (1975).

[7] P. C. Rout, D. R. Chakrabarty, V. M. Datar, Suresh Kumar, E. T. Mirgule, A. Mitra, V. Nanal, S. P. Behera, and V. Singh, Phys. Rev. Lett. **110**, 062501 (2013).

[8] S. F. Mughabghab and C. Dunford, Phys. Rev. Lett. **81**, 4083 (1998).

[9] G. Nebbia, K. Hagel, D. Fabris, Z. Majka, J. B. Natowitz, R. P. Schimitt, B. Sterling, G. Mouchaty, G. Berkowitz, K. Strozewski, G. Viesti, P. L. Gonthier, B. Wilkins, M. M. Namboodiri, and H. Ho, Phys. Lett. B **176**, 20 (1986).

[10] K. Hagel, D. Fabris, P. Gonthier, H. Ho, Y. Lou, Z. Majka, G. Mouchaty, M. N. Namboodiri, J. B. Natowitz, G. Nebbia, R. P. Schmitt, G. Viesti, R. Wada, and B. Wilkins, Nucl. Phys. A **486**, 429 (1988).

[11] M. Gonin, L. Cooke, K. Hagel, Y. Lou, J. B. Natowitz, R. P. Schmitt, B. Srivastava, W. Turmel, H. Utsunomiya, R. Wada, B. Fornal, G. Nardelli, G. Nebbia, G. Viesti, R. Zanon, G. Prete, P. Gonthier, and B. Wilkins, Phys. Lett. B **217**, 406 (1989).

[12] M. Gonin, L. Cooke, K. Hagel, Y. Lou, J. B. Natowitz, R. P. Schmitt, S. Shlomo, B. Srivastava, W. Turmel, H. Utsunomiya, R. Wada, G. Nardelli, G. Nebbia, G. Viesti, R. Zanon, B. Fornal, G. Prete, K. Niita, S. Hannuschke, P. Gonthier, and B. Wilkins, Phys. Rev. C **42**, 2125 (1990).

[13] R. Wada, D. Fabris, K. Hagel, G. Nebbia, Y. Lou, M. Gonin, J. B. Natowitz, R. Billerey, B. Cheynis, A. Demeyer, D. Drain, D. Guinet, C. Pastor, L. Vagneron, K. Zaid, J. Alarja, A. Giorni, D. Heuer, C. Morand, B. Viano, C. Mazur, C. Ngo, S. Leray, R. Lucas, M. Ribrag, and E. Tomasi, Phys. Rev. C **39**, 497 (1989).

[14] M. Prakash, J. Wambach, and Z. Y. Ma, Phys. Lett. B **128**, 141 (1983).

[15] R. W. Hasse and P. Schuck, Phys. Lett. B **179**, 313 (1986).

[16] S. Shlomo and J. B. Natowitz, Phys. Lett. B **252**, 187 (1990).

[17] S. Shlomo and J. B. Natowitz, Phys. Rev. C **44**, 2878 (1991).

[18] J. N. De, S. Shlomo, and S. K. Samaddar, Phys. Rev. C **57**, 1398 (1998).

[19] B. J. Fineman, K. T. Brinkmann, A. L. Caraley, N. Gan, R. L. McGrath, and J. Velkovska, Phys. Rev. C **50**, 1991 (1994).

[20] D. Fabris, E. Fioretto, G. Viesti, M. Cinausero, N. Gelli, K. Hagel, F. Lucarelli, J. B. Natowitz, G. Nebbia, G. Prete, and R. Wada, Phys. Rev. C **50**, 1261(R) (1994).

[21] A. L. Caraley, B. P. Henry, J. P. Lestone, and R. Vandenbosch, Phys. Rev. C **62**, 054612 (2000).

[22] A. Chbihi, L. G. Sobotka, N. G. Nicolis, D. G. Sarantites, D. W. Stracener, Z. Majka, D. C. Hensley, J. R. Beene, and M. L. Halbert, Phys. Rev. C **43**, 666 (1991).

[23] G. Nebbia, D. Fabris, A. Perin, G. Viesti, F. Gramegna, G. Ptete, L. Fiore, V. Paticchio, F. Lucatelli, B. Chambon, B. Cheynis, D. Drain, A. Giorni, A. Lleres, and J. B. Viano, Nucl. Phys. A **578**, 285 (1994).

[24] K. Yoshida, J. Kasagi, H. Hama, M. Sakurai, M. Kodama, K. Furutaka, K. Ieki, W. Galster, T. Kubo, M. Ishihara, and A. Galonsky, Phys. Rev. C **46**, 961 (1992).

[25] G. Dietze and H. Klein, PTB-ND-22 Report (1982).

[26] F. Puhlhofer, Nucl. Phys. A **280**, 267 (1976).

[27] S. Cohen, F. Plasil, and W. J. Swiatechi, Ann. Phys. (NY) **82**, 557 (1974).

[28] D. Wilmore and P. E. Hodgson, Nucl. Phys. **55**, 673 (1964); P. E. Hodgson, Ann. Rev. Nucl. Sci **17**, 1 (1967).

[29] P. Moller, J. R. Nix, W. D. Myers, and W. J. Swiateki, At. Data Nucl. Data Tables **59**, 185 (1995).

[30] K. H. Schmidt, H. Delagrange, J. P. Dufour, N. Cgtrjan, and A. Fleury, Z. Phys. A: At. Nucl. **308**, 215 (1982).

[31] R. J. Charity, Phys. Rev. C **82**, 014610 (2010).

[32] P. F. Bortignon and C. H. Dasso, Phys. Lett. B **189**, 381 (1987).

[33] D. R. Chakrabarty, S. K. Rathi, V. M. Datar, Suresh Kumar, E. T. Mirgule, A. Mitra, and H. H. Oza, Nucl. Phys. A **712**, 23 (2002).

[34] A. R. Junghans, M. de Jong, H. G. Clerc, A. V. Ignatyuk, G. A. Kudyaev, and K. H. Schmidt, Nucl. Phys. A **629**, 635 (1998).

[35] V. A. Plujko, O. M. Gorbachenko, and I. M. Kadenko, Int. J. Mod. Phys. E **16**, 570 (2007).